Supernova 1987A:30 years later - Cosmic Rays and Nuclei from Supernovae and their aftermaths
Proceedings IAU Symposium No. 331, 2017
A. Marcowith, M. Renaud, G. Dubner, A. Ray & A. Bykov, eds.

doi:10.1017/S174392131700641X

Diagnostics of the Supernova Engine

Chris L. Fryer[1], Carola Ellinger[1], Patrick A. Young[2] and Gregory Vance[2]

[1]CCS-2, MS D409, Los Alamos Naitonal Laboratory, Los Alamos, NM 87544
email:*fryer@lanl.gov*

[2]Department of Physics and Astronomy, Arizona State University, P.O. Box 1504, Tempe, AZ 85287-1504

Abstract. The standard engine behind core-collapse supernovae is continuously evolving with increasingly detailed models. At this time, most simulations focus on an engine invoking turbulence above the proto-neutron star, sometimes termed the "convection-enhanced" engine. Here we review this engine and why it has become the standard for normal supernovae, focusing on a wide set of observations that provide insight into the supernova engine.

Keywords. supernova, neutron star, black holes

1. Introduction

Supernovae are among the most powerful explosions in the universe with kinetic energies in excess of 10^{51} erg†. Even as the neutron was just being characterized, it was realized that this energy could be achieved by having the core of a massive star collapse down to a core composed entirely of neutrons (Baade & Zwicky 1934). Ultimately, this collapse releases over 10^{53} erg of gravitational potential energy and only 1% of this energy is needed to drive the explosion.

This is easier said than done, and scientists have been working to achieve this 1% efficiency for the past 80 years. At this point in time, the arising favored model arguing that convection above the proto-neutron star increases the efficiency at which the potential energy released in the collapse is able to drive a strong mass ejection. The broad community now has a series of simulations that produce explosions. In this paper, we review this engine, comparing results of this engine with the current suite of observations. Leading alternative engines invoking magnetically dominated flows are much less sophisticated at the moment and hence, the comparison to observations is less constraining. But we will discuss these comparisons where possible. Section 2 provides a brief overview of the engine followed by a series of sections reviewing the supernova energetics (section 3), remnant masses (section 4), supernova asymmetries including observations of ejecta remnants(section 5).

2. Engine Models

Supernovae are produced at the end of a star's life when the central iron core collapses in on itself. The iron core is produced through a succession of burning phases where the ashes of the previous phase of nuclear burning becomes the fuel for the next phase as the core contracts and heats up. The iron core is supported by thermal and electron

† 10^{51} erg has been termed a FOE (for Fifty One Erg) by Hans Bethe. This unit is also termed a Bethe

degeneracy pressure. As silicon shell burning adds mass to the iron core, it contracts under its own weight. When the contraction creates sufficiently high densities and temperatures to allow electron capture onto protons, the collapse begins. Electron capture removes degeneracy pressure, causing the core to contract further that, in turn, increases the electron capture rate. In addition, the temperatures in the core become sufficiently high to cause the iron atoms to dissociate, removing thermal pressure. Very quickly, the stable neutron star evolves into a runaway collapse, imploding at nearly free-fall.

The collapse continues until the core reaches nuclear densities when nuclear forces and neutron degeneracy pressure dramatically increase the pressure, causing the core to bounce. Initial models argued this "bounce" would drive the explosion (Colgate & Johnson 1960). However, most of the energy in the bounce is stored in neutrinos and as the shock moves sufficiently outward to become optically thin to neutrinos, it quickly stalls. At this point, the interior of the star consists of a collapsed core (termed the proto-neutron star) $\sim 30 - 50\,\mathrm{km}$ in extent and the material from the failed bounce shock extending to $\sim 100 - 300\,\mathrm{km}$.

With the bounce shock failing, the proposed supernova engine evolved. Most of the gravitational potential energy released is deposited as thermal energy in the core. The photons at these densities have mean free paths smaller than a nanometer and can not transport energy. However, for the temperatures in the core, most of the energy is in neutrinos. Even with the extremely low matter-interaction cross-section of neutrinos, the neutrinos are also trapped, but the optical depth is low enough that the neutrinos can diffuse out, heating the failed shock. The next evolution of the supernova model argued that this neutrino heating could revive the shock (Colgate & White 1966).

Although simple prescriptions for this neutrino energy deposition did revive the shock, detailed 1-dimensional models were unable to produce a large enough neutrino flux to drive the explosion. To increase this flux, scientists looked into convective instabilities. Although the entropy gradient suggests a stable profile within the neutron star, the emission at the neutrinosphere (upper edge of the proto-neutron star) produces a composition gradient that is Ledoux unstable (Epstein 1979). This gradient arises as electron neutrinos from electron capture escape, allowing the electron fraction to decrease dramatically. This lepton instability criterion is:

$$(\partial\rho/\partial S)_{P,Y_l}\, dS/dr + (\partial\rho/\partial Y_l)_{P,S}\, dY_l/dr > 0, \tag{2.1}$$

where ρ is the density, S is the entropy, P is the pressure, and Y_l lepton fraction. As this instability builds, it can expand to cover a large fraction of the proto-neutron star(Burrows & Lattimer 1988, Keil *et al.* 1996), but the increase in flux is typically insufficient to drive an explosion.

While this was being studied, supernova 1987A exploded. This supernova both confirmed many of the theoretical models while also bringing new issues currently unexplained by the models. The detection of neutrinos from the core proved that the explosion occured during the collapse to a neutron star (Bionta *et al.* 1987, Hirata *et al.* 1987). But the ^{56}Ni decay gamma-rays appeared much earlier than scientists expected (Pinto & Woosley 1988). ^{56}Ni is produced in the innermost supernova ejecta where silicon is burned into ^{56}Ni as the shock plows through it. 1-dimensional models argued that it would take over 200 d for the ^{56}Ni to be uncovered enough such that the gamma-rays produced in its decay would leak out of the star. Observers detected those gamma-rays at 150 d. Scientists realized that this ^{56}Ni must be mixed out in the star. Additional evidence argued for extensive mixing, e.g. the broad lines seen in the iron lines iron lines produced from ^{56}Ni decay required that the ^{56}Ni be extensively mixed.

https://doi.org/10.1017/S174392131700641X Published online by Cambridge University Press

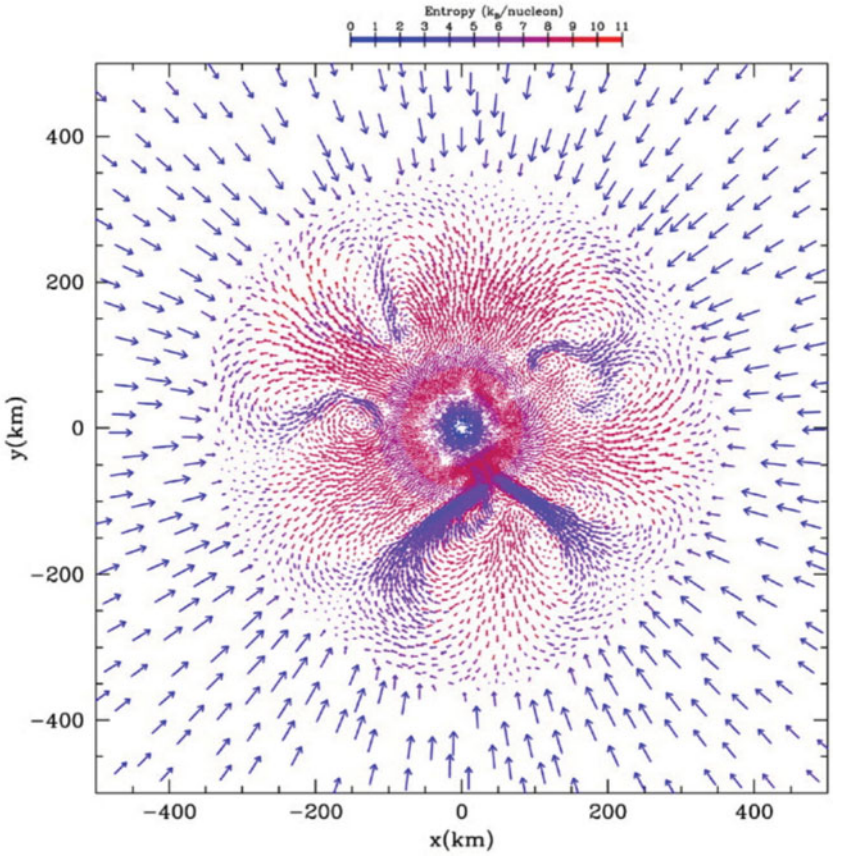

Figure 1. Slice of a 3-dimensional simulation of the core collapse engine. The colors denote the entropy and the length and direction of the arrows correspond to the magnitude and direction of the material. The neutron star is roughly 50 km in size and the bounce shock stalled at just above 200 km. Material from the infalling star piles up at the stalled shock until it drives a downflow - like dust motes on a pond surface. These downflows stream down to the proto-neutron star where they are either heated and begin to rise in an upflow or accrete onto the proto-neutron star (Fig. 2, Fryer & Warren 2002).

What causes this mixing? The supernova shock is unstable to Rayleigh-Taylor convection, but scientists studying this mixing in multi-dimensional codes were unable to achieve the high level of mixing observed (e.g. Herant *et al.* 1992). Scientists began to review the instabilities in the stalled shock region and the supernova engine began to evolve further. The bounce shock heats and compresses the star as it moves through it. In the strong shock limit, the pressure and density after being shocked are:

$$P_{\rm shock} = (\gamma + 1)/2 \rho_{\rm star} v^2 \tag{2.2}$$

and

$$\rho_{\rm shock} = (\gamma + 1)/(\gamma - 1) \rho_{\rm star} \tag{2.3}$$

where γ is the adiabatic index of the stellar material (we can assume a radiation dominated gas, $\gamma = 4/3$), $\rho_{\rm star}$ is the density of the imploding stellar material and v is the relative velocity of the shock and the infalling material: $v \approx v_{\rm shock} + v_{\rm free-fall}$. For a

https://doi.org/10.1017/S174392131700641X Published online by Cambridge University Press

radiation dominated gas, the entropy (S) of material is:

$$S = S_0 \rho_{\rm star}^{-1/4} v^{3/2} \tag{2.4}$$

where we have subsumed any constants into S_0. If $\rho_{\rm star} \propto r^{-3}$ and $v \propto r^{-1/2}$, the entropy would be constant with respect to r and we would expect a stable stratification. However, typically the density falls of less steeply and the velocity decreases more steeply such that there is at least a portion of this failed shock region that is unstable to Rayleigh-Taylor instabilities. In addition, neutrino heating from the proto-neutron star would further drive the Rayleigh-Taylor instability. This convection, driven by limitations in the current engine and the evidence of mixing in SN 1987A, became the next step in the evolution of the supernova engine.

Figure 1 shows a slice of a 3-dimensional simulation of this convective engine. High entropy bubbles rise as low entropy downflows move from the top of the stalled shock down to the neutrino heating region (this region is termed the gain region because the net energy gained by neutrino deposition is large than that lost through neutrino emission). This convection helps the explosion in 2 ways: 1) by allowing material that has piled up at the top of the stalled shock to flow down toward the proto-neutron star, it reduces the pressure the convective region must overcome to drive an explosion, 2) by allowing the material heated by neutrinos to rise, its thermal energy is converted to kinetic energy, allowing it to cool before it begins to lose its energy through neutrino emission. With this engine, scientists began to produce explosions (Herant *et al.* 1994, Buras *et al.* 2006, Lentz *et al.* 2015).

As most groups confirming this engine with detailed models, there is little disagreement that this convection plays an important role. However, there are disagreements on the nature of the convection: for instance, is the matter moving because of Rayleigh-Taylor convection or the standing accretion shock instability (SASI). One way to decide this argument is based on the growth time of these instabilities. The Rayleigh-Taylor growth time ($\tau_{\rm conv}$) can be estimated by the Brunt-Väisäla frequency: $\tau_{\rm conv} = (|1/\omega^2|)^2$ where ω is the Brunt-Väisäla frequency:

$$\omega^2 = g/\rho(\partial\rho/\partial S)_P(\partial S/\partial r) \approx (1/S)(GM_{\rm enclosed}/r^2)(\Delta S/\Delta r) \tag{2.5}$$

with the gravitational acceleration $g = GM_{\rm enclosed}/r^2$, S is the entropy, P is the pressure, r is the radius and $M_{\rm enclosed}$ is the enclosed mass. For the conditions of our failed bounce, $\Delta S/S \approx 0.2$, $g \approx 1.5 \times 10^{12}$cm s^{-2}, and $\Delta r = 10^7$cm, the Rayleigh-Taylor growth time is 2 ms. The standing accretion shock instability has a much slower growth time ~ 100 ms (Houck & Chevalier 1992, Blondin *et al.* 2003) and, unless the entropy gradient can be flattened (Rayleigh-Taylor could possible do this quickly), it should not dominate the material motion (Fryer & Young 2007).

Note that this supernova engine is not robust. It depends sensitively on our ability to model the convection as well as the details of the microphysics. But as we shall discuss in the next section, this appears to be what is needed to match nature.

Alternative engines exist. Among the most popular are engines driven by magnetic fields. The favored engine behind long-duration gamma-ray bursts argues that the collapsing core does not explode with this convection-enhanced engine and the core ultimately collapses to form a black hole. If the star is rotating fast enough, a disk will form around this black hole and this "collapsar" engine argues that strong magnetic fields will develop in this disk, producing a jet that drives the explosions (Woosley 1993). Scientists have also invoked this magnetically-driven disk engine for supernovae. One of the difficulties of this engine is getting enough rotation. The specific angular momentum of massive stars increases with radius. The collapsar engine leveraged this fact, allowing the

https://doi.org/10.1017/S174392131700641X Published online by Cambridge University Press

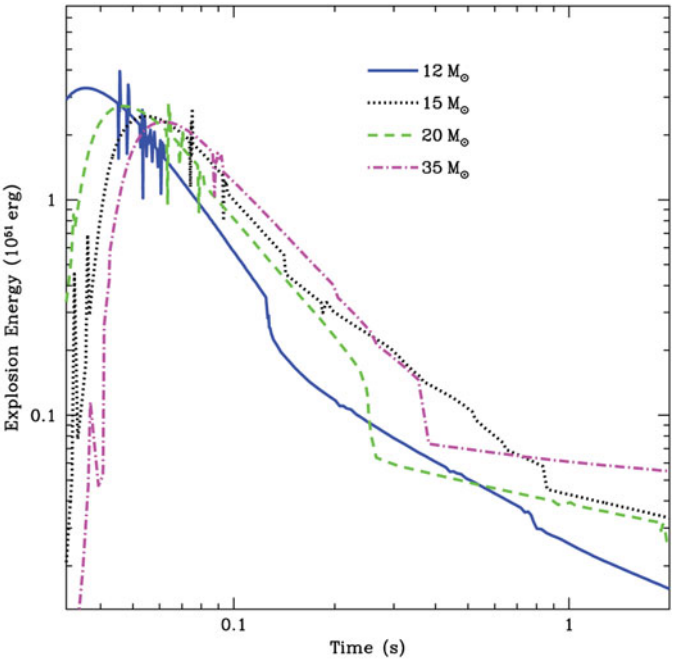

Figure 2. Supernova energy for 3 different models as a function of the time after collapse that the shock is launched. As the density of the infalling material decreases, less energy is needed to drive an explosion, but the resultant supernova explosion energy is less (Fig.1 of Fryer *et al.* 2012.)

low angular momentum material accrete onto the black hole before forming a disk. The specific angular momentum ($j_{\rm star}$)needed to form a disk is:

$$j = (GM_{\rm PNS} r_{\rm disk})^{1/2} \tag{2.6}$$

where G is the gravitational constant, $M_{\rm PNS}$ is the mass within the disk (roughly the proto-neutron star mass) and $r_{\rm disk}$ is the disk radius. For a 100 km disk around 1.5 $M_\odot$ proto-neutron star, the angular momentum need is $4\times10^{16}{\rm cm}^2\ {\rm s}^{-1}$. This is only produced in rapidly spinning stars that neglect many physics processes that couple the neutron star (note that these stars would produced sub ms pulsars. Given that most pulsars are spinning at roughly 100 ms, such fast rotations are rare.

3. Supernova Energies

As we discussed in the introduction, the large, 1-3 foe, energies observed in supernovae is what prompted the first proposal of a core-collapse engine. But the distribution of the observed supernova energies place even stronger constraints on the engine and mark one of the strongest successes of the convective engine. The convective engine persists until the pressure at the edge of the failed shock that marks the edge of the convective region can overcome the ram pressure of the infalling star. The pressure in the convective region ($P_{\rm convection}$) assuming a roughly constant entropy region is Fryer *et al.* 2012:

$$P_{\rm convection}(r) = [0.25 S_0 M_{\rm NS} G S^{-1}(1/r - 1/r_{\rm shock}) + P_{\rm shock}^{1/4}]^4 {\rm erg\,g}^{-1} \tag{3.1}$$

where the pressure in the shock ($P_{\rm shock}$) is:

$$P_{\rm shock}(r) = 1/2 \rho_{\rm shock} v_{\rm free-fall}^2. \tag{3.2}$$

https://doi.org/10.1017/S174392131700641X Published online by Cambridge University Press

where $S_0 = 1.5 \times 10^{-11}$, $M_{\rm NS}$ is the mass of the neutron star, G is the gravitational constant, r and $r_{\rm shock}$ are the radii in the convective region and of the shock (edge of convective region) respectively, $\rho_{\rm shock}$ is the density of the shocked infalling materiall and $v_{\rm free-fall}$ is the free fall velocity. The specific energy ($u_{\rm convection}$) in this convective region is then:

$$u_{\rm convection}(r) = 3[4.7 \times 10^8 M_{\rm NS}(M_\odot)(S/10 k_{\rm B}\,{\rm nucleon}^{-1}) \quad (3.3)$$

$$\times(r^{-1}(10\,{\rm km}) - r_{\rm shock}^{-1}(10\,{\rm km})) + 1.2 \times 10^6 M_{\rm NS}^{1/8}(M_\odot) \quad (3.4)$$

$$\times(\dot{M}_{acc}^{1/4}({\rm M_\odot s^{-1}})({\rm r_{shock}^{-5/8}(200\,km)}]^4 {\rm erg\,cm^{-3}} \quad (3.5)$$

where $\dot{M}_{acc}$ is the accretion rate of the imploding star onto the convective region. The energy in this region depends both on this accretion rate, the entropy in the region, and the radius of the shock. If we assume the engine turns off once the explosion is launched because the density becomes too low to absorb any neutrinos, we can use simulation-guided values for the entropy and shock radius to determine the explosion energy as a function of explosion time (Fryer *et al.* 2012). Because the accretion rate decreases with time, the energy decreases with time. The supernova energy as a function of time and progenitor is shown in Figure 2. Note that this estimate is likely to be a lower limit because most simulated explosions are not complete; material continues to fall onto the neutron star after the supernova explosion. A fraction of this "fallback" material can absorb energy and become part of the explosion.

One of the energy requirements placed on the core-collapse model is to explain why most supernovae have energies that are 1% of the 10^{53} erg released in the collapse. This convective model provides a natural explanation for this limit - if the energy got more than a few foe, the shock would launch, turning off the engine. The energy from magnetic engine models can not explain this observational fact. Currently, practitioners of magnetic-field models argue the progenitor dictates the energy distribution, e.g. the distribution of rotations is such that most explosions extract 1% of the total energy released - the model is tuned to fit the answer. Despite the strengths of the convective engine, its limitation is that it can not explain extremely energetic supernova, e.g. hypernovae. In cases where there is considerable fallback, the convective engine can produce more energetic explosions, but it is unlikely that this is sufficient to explain hypernovae and a different engine, e.g. collapsar, is required to explain really powerful explosions.

4. Compact Remnants

The compact remnant mass distribution also places strong constraints on the supernova engine. When the convective engine was first proposed, compact mass distributions were believed to be delta functions, with neutron stars masses very close to $1.4\,{\rm M_\odot}$ and black hole masses of $\sim 7\,{\rm M_\odot}$ (Thorsett & Chakrabarty 1999). Defying observational evidence, the convective engine predicted a range of masses (Fryer & Kalogera 2001). We now know that there are a range of compact remnant masses, confirming this prediction of the convective engine. However, the convective engine did not predict the observed mass gap between neutron star and black hole masses. This gap, if it represents the birth mass distribution, has important implications on the convective engine and by constraining the engine to either very strong or very weak explosions (Fryer *et al.* 2012, Belczynski *et al.* 2012). Fig. 3 plots both predicted remnant distributions of remnants in binaries along with the observed distribution. Note, however, that scientists studying binary accretion have argued that the compact remnant can accrete considerable mass post-formation and

https://doi.org/10.1017/S174392131700641X Published online by Cambridge University Press

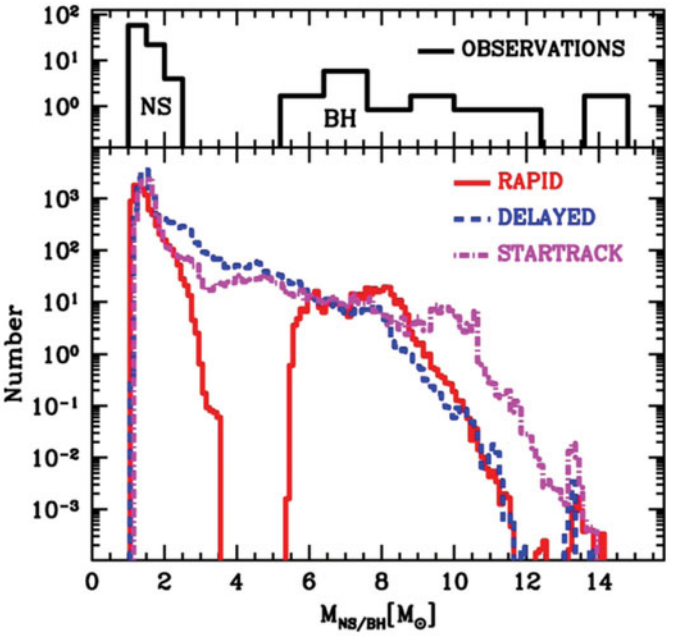

Figure 3. Mass distribution of compact remnants both from theoretical models and in observations. Compact remnant masses are only determined for systems in binaries and these theoretical models are produced through binary population studies (Fig. 1. of Belczynski *et al.* 2012.)

that no gap exists in the birth distribution of compact remnants (Fragos & McClintock 2015).

Magnetic field models have yet to explain these observations.

5. Supernova Asymmetries

For 1987A, the early emergence of the gamma-rays from ^{56}Ni decay and the spectral line widths drove the initial studies of the convective engine. But there is further evidence that supernovae are asymmetric. First and foremost, the pulsar velocity distribution suggests that neutron stars are born with a "kick" that, in some cases, can exceed $1000\,\mathrm{km\,s^{-1}}$. In addition, a straightforward explanation of the large polarization seen in some core-collapse supernovae is that the explosions driving these supernovae are asymmetric (see Hungerford *et al.* 2003 for a review). The ejecta remnants also show evidence for asymmetries. In the Cassiopeia A remnant, there is a visible "jet-like" structure in the silicon ejecta (Hwang *et al.* 2004). However, as we shall discuss below, the titanium distribution tells a very different story.

Before we discuss the latest results on Cassiopeia A, let's review the theoretical models. Not long after the first succesful supernova explosions were produced with the convective engine, scientists argued that the Rayleigh-Taylor convection would develop into low modes (as seen in many simulations of Rayleigh-Taylor convection) and, in some cases, could produce the large kicks (Herant 1995). The strongest convective cycles in the standing accretion shock instability are low mode and this model could produce asymmetric explosions to explain pulsar kicks. SN 1987A appears to be dominated by a single mode and such low modes are possible in the convective engine.

Jet-like explosions are much more difficult to explain. One way to make bimodal explosions is by collapsing a rotating star. The criterion for instability in a rotating star

https://doi.org/10.1017/S174392131700641X Published online by Cambridge University Press

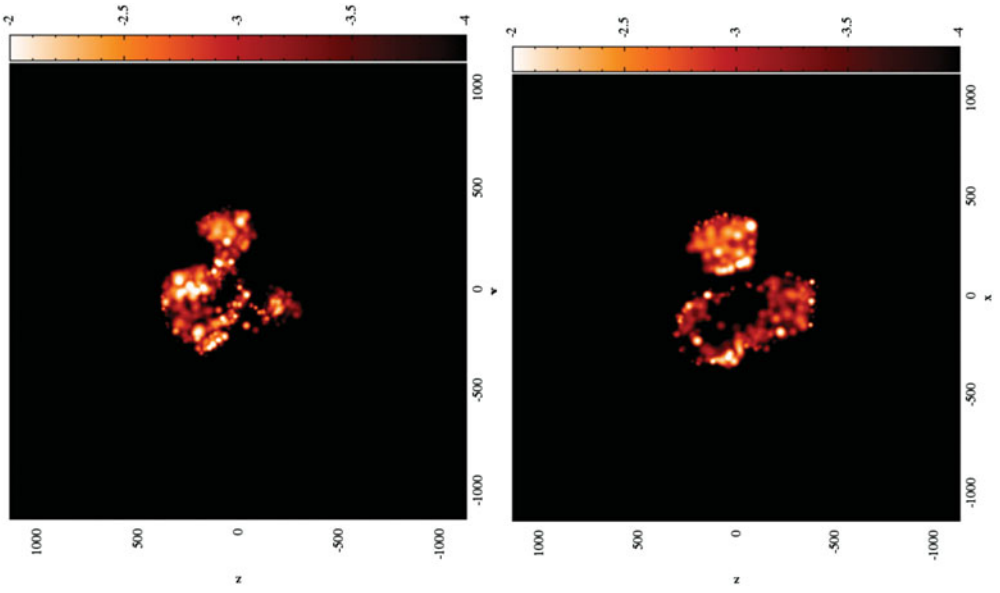

Figure 4. Color plots of two slices from a 3-dimensional supernova explosion of the ^{44}Ti/iron ratio. The low-mode convection produces low-mode clumps of ^{44}Ti similar to that observed in Cassiopeia A.

is:

$$g/\rho[(d\rho/dr)_S - d\rho/dr] - 1/r^3 dj^2/dr > 0. \quad (5.1)$$

where g is the gravitational acceleration, ρ is the density, j is the angular momentum, S is the entropy and r is the radius. If the angular momentum increases at larger radii (which it does for most stars), there is a stabilizing force against convection. The angular momentum is high along the spin equatorial plane, but convection can still occur along the rotation axis. The convective engine then produces an explosion that is much stronger along the rotation axis, even without magnetic fields (Fryer & Heger 2000). Of course, with magnetic fields, a range of jet models exist.

It is worth mentioning that the most extremeley asymmetric core-collapse events are hypernovae which not only appear jet-like, but also much too energetic to explain with the convective engine. It is likely that some mechanism, like the black-hole accretion disk magneto-hydrodynamic engines explain these explosions.

But let's return to what we believe to be normal supernova asymmetries - like the jet-like structure in Cassiopeia A. Although the remnant community argued, and in some cases still argues, that this jet structure must be caused by the engine (Hwang *et al.* 2004), analysis of the remnant can be difficult. Understanding the emission from excited lines requires that the material be heated, shocked by either the forward or reverse shock in the explosion. Because of this, the circumstellar medium can alter the shape and an alternate explanation for this jet-like feature is that the circumstellar medium is asymmetric (Blondin *et al.* 1996).

The NuSTAR satellite promised a more direct probe of the asymmetries in Cassiopeia A. ^{44}Ti is produced in the innermost ejecta of a supernova along with the ^{56}Ni. Its 60 year half-life make it ideally suited to probe the distribution of this ejecta in supernova remnants. Figure 4 shows the ^{44}Ti/iron ratio for a convectively-driven supernova. The low-mode convection produces an explosion with low-mode asymmetries which grow as the shock plows through the star.

https://doi.org/10.1017/S174392131700641X Published online by Cambridge University Press

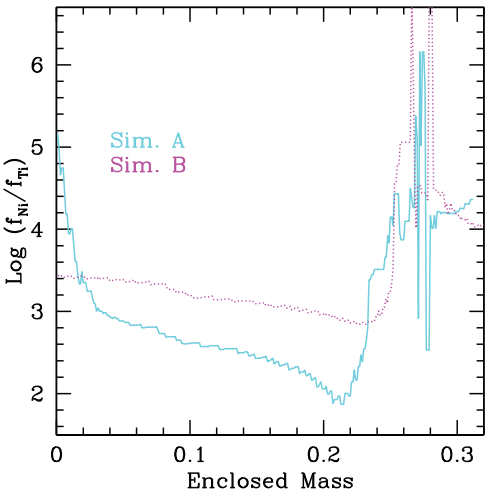

Figure 5. Ratio of ^{44}Ti to ^{56}Ni production in two supernova simulations. The ^{56}Ni production is fairly insensitive to the explosion details, but the ^{44}Ti production depends upon the progenitor structure, shock strength and electron fraction, making it an ideal probe of the explosion physics.

The NuSTAR satellite, with a wavelength coverage from a few to 80 keV, can directly observe 2 decay lines from ^{44}Ti. The strength of this probe is twofold: first, the ^{44}Ti is produced solely in the innermost ejecta with negligible mass fraction in the star or circumstellar medium (it is sometimes difficult to distinguish iron made in the supernova and iron already existing in the star) and second, we can observe all of the ^{44}Ti and, aside from small possible changes in the decay timescale due to excited states, the ^{44}Ti measurement is a clean, direct measurement of the ^{44}Ti. What we observed with a low mode, but not bimodal, ejection (Grefenstette *et al.* 2014, Grefenstette *et al.* 2017). The predictions of the convective model were correct. Although there are some arguments for jet jitter causing the observed structure, it appears that a magnetic-driven engine is not behind the explosion behind the Cassiopeia A remnant.

Figure 5 shows the ^{44}Ti/^{56}Ni ratio for two different supernova explosions. The strong sensitivity of the ^{44}Ti production to the characteristics of the supernova explosion make it an ideal probe of this explosion. We have only touched the surface of what we can learn from these explosions. Perhaps these comparisons will cause a new evolution in the model.

6. Summary

We have reviewed the evolution of the core-collapse engine into a convectively driven engine. Based primarily upon the fact that supernova are energetic and asymmetries seemed necessary to explain mixing, the convective engine explains naturally the preponderence of normal-energy, few foe, supernovae, predicted the range of remnant masses, and correctly predicted the asymmetries in the Cassiopeia A remnant. Alternative engine, e.g. magnetically driven engines, are needed to explain the most energy supernovae (e.g. hypernovae), but these engines have not been able to explain most of the observations for normal supernovae. Because of this, the convective-driven engine has become the favored mechanism for normal supernovae.

https://doi.org/10.1017/S174392131700641X Published online by Cambridge University Press

References

Baade, W. & Zwicky, F. 1934, *Phys. Rev.*, 46, 76
Bionta, R. M., Blewitt, G., Bratton, C. B., Casper, D., & Ciocio, A. 1987, *PRL*, 58, 1494
Blondin, J. M., Lundqvist, P., & Chevalier, R. A. 1996, *ApJ*, 472, 257
Blondin, J. M., Mezzacappa, A., & DeMarino, C. 2003, *ApJ*, 584, 971
Buras, R., Rampp, M., Janka, H.-T., & Kifonidis, K. 2006, *A&A*, 447, 1049
Burrows, A. & Lattimer, J. M. 1988, *Phys. Rep.*, 163, 51
Colgate, S. A. & Johnson, M. H. 1960, *PRL*, 5, 235
Colgate, S. A. & White, R. H. 1966, *ApJ*, 143, 626
Epstein, R. I. 1979, *ApJ*, 188, 305
Fragos, T. & McClintock, J. E. 2015, *ApJ*, 800, 17
Fryer, C. L. & Heger, A. 2000, *ApJ*, 541, 1033
Fryer, C. L. & Kalogera, V. 2001, *ApJ*, 554, 548
Fryer, C. L. & Warren, M. 2002, *ApJ*, 574, L65
Fryer, C. L. & Young, P. A. 2007, *ApJ*, 659, 389
Fryer, C. L., Belczynski, K., Wiktorowicz, G., Dominik, M., Kalogera, V., & Holz, D. 2012, *ApJ*, 749, 91
Grefenstette, B. W. *et al.* 2014, *Nature*, 506, 339
Grefenstette, B. W. *et al.* 2017, *ApJ*, 834, 19
Herant, M., Benz, W., & Colgate, S. 1992, *ApJ*, 395, 642
Herant, M., Benz, W., Hix, W. R., Fryer, C. L., & Colgate, S. A. 1994, *ApJ*, 435, 339
Herant, M. 1995, *Phys. Rep.*, 256, 117
Houck, J. C., & Chevalier, R. A. 1992 *ApJ*, 395, 592
Hirata, K., Kajita, T., Koshiba, M., Nakahata, M., & Oyama, Y. 1987, *PRL*, 58, 1490
Hungerford, A. L., Fryer, C. L., & Warren, M. S. 2003, *ApJ*, 594, 390
Hwang, U. *et al.* 2004 2004, *ApJ*, 615, L117
Keil, W., Janka, H.-T., & Müller, E. 1996, *ApJ*, 473, L111
Lentz, E. J., Bruenn, S. W., Hix, W. R., Mezzacappa, A., Messer, O. E. B., Endeve, E., Blondin, J. M., Harris, J. A., Marronetti, P., & Yakunin, K. N. 2015, *ApJ*, 807, L31
Pinto, P. A. & Woosley, S. E. 1988, *ApJ*, 329, 820
Thorsett, S. E. & Chakrabarty, D. 1999, *ApJ*, 512, 288
Woosley, S. E. 1993, *ApJ*, 405, 273

https://doi.org/10.1017/S174392131700641X Published online by Cambridge University Press